Inorganic Chemistry
Article

Inorg. Chem. **2010**, *49*, 1481–1486 **1481**
DOI: 10.1021/ic901758s

Synthesis and Characterization of an Asymmetric, Linear, Trinuclear Manganese(II) Complex

Cristina M. Coates,[†,||] Stephanie R. Fiedler,[‡,||] T. Laura McCullough,[†] Thomas E. Albrecht-Schmitt,[§] Matthew P. Shores,[‡] and Christian R. Goldsmith*[,†]

[†]*Department of Chemistry & Biochemistry, Auburn University, Auburn, Alabama 36849,* [‡]*Department of Chemistry, Colorado State University, Fort Collins, Colorado 80523, and* [§]*Department of Civil Engineering and Geological Sciences, University of Notre Dame, Notre Dame, Indiana 46556.* [||] *These authors contributed equally to this work*

Received September 3, 2009

After prolonged heating in acetonitrile, a highly asymmetric, trinuclear manganous complex self-assembles from $MnCl_2$ and bis(2-pyridylmethyl)-1,2-ethanediamine (bispicen). The central Mn(II) ion is bridged to the terminal metal ions in the molecule by single chloride anions. The organic ligands each bind to a single Mn(II) ion. The central Mn(II) and only one of the terminal Mn(II) ions are six-coordinate and bound to bispicen ligands. The remaining terminal Mn(II) ion is coordinated by a tetrahedral array of chloride anions, endowing the trinuclear cluster with a high degree of asymmetry. Variable temperature magnetic measurements are consistent with an $S = 5/2$ system, indicating net antiferromagnetic coupling.

Introduction

Novel polynuclear manganese complexes have been sought for their potential to act as single-molecule magnets (SMMs)[1−4] and models for the manganese core of the oxygen evolving complex (OEC) in Photosystem II.[5−7] The development of novel SMMs would allow for the production of smaller and higher density memory storage devices. Functional OEC mimics could provide means to store solar energy, thereby enabling alternative fuel technologies. Efforts commensurate with the potential benefits have been expended in attempts to correlate the structural characteristics of polynuclear manganese cage complexes to their physical and chemical properties.[1−14]

Trinuclear manganese structures can both serve as precursors to higher nuclearity clusters and exhibit intriguing magnetic properties of their own. These trinuclear cage complexes have Mn(II) and Mn(III) ions arrayed in either triangular (close structure)[6,7,15−17] or linear (open structure) geometries.[6,7,18−25] Most of these trinuclear compounds are symmetric, with at least two of the three manganese ions

*To whom correspondence should be addressed. E-mail: crgoldsmith@auburn.edu.

(1) Sessoli, R.; Tsai, H. L.; Schake, A. R.; Wang, S.; Vincent, J. B.; Folting, K.; Gatteschi, D.; Christou, G.; Hendrickson, D. N. *J. Am. Chem. Soc.* **1993**, *115*, 1804–1816.
(2) Sessoli, R.; Gatteschi, D.; Caneschi, A.; Novak, M. A. *Nature* **1993**, *365*, 141–143.
(3) Milios, C. J.; Vinslava, A.; Wernsdorfer, W.; Moggach, S.; Parsons, S.; Perlepes, S. P.; Christou, G.; Brechin, E. K. *J. Am. Chem. Soc.* **2007**, *129*, 2754–2755.
(4) Milios, C. J.; Inglis, R.; Vinslava, A.; Bagai, R.; Wernsdorfer, W.; Parsons, S.; Perlepes, S. P.; Christou, G.; Brechin, E. K. *J. Am. Chem. Soc.* **2007**, *129*, 12505–12511.
(5) Boskovic, C.; Brechin, E. K.; Streib, W. E.; Folting, K.; Bollinger, J. C.; Hendrickson, D. N.; Christou, G. *J. Am. Chem. Soc.* **2002**, *124*, 3725–3736.
(6) Mukhopadhyay, S.; Mandal, S. K.; Bhaduri, S.; Armstrong, W. H. *Chem. Rev.* **2004**, *104*, 3981–4026.
(7) Kessissoglou, D. P. *Coord. Chem. Rev.* **1999**, *185−186*, 837–858.
(8) Hoshiko, J. A.; Wang, G.; Ziller, J. W.; Yee, G. T.; Heyduk, A. F. *Dalton Trans.* **2008**, 5712–5714.
(9) Sieber, A.; Foguet-Albiol, D.; Waldmann, O.; Ochsenbein, S. T.; Bircher, R.; Christou, G.; Fernandez-Alonso, F.; Mutka, H.; Güdel, H. U. *Inorg. Chem.* **2005**, *44*, 6771–6776.
(10) Stamatatos, T. C.; Foguet-Albiol, D.; Poole, K. M.; Wernsdorfer, W.; Abboud, K. A.; O'Brien, T. A.; Christou, G. *Inorg. Chem.* **2009**, *48*, 9831–9845.
(11) Stamatatos, T. C.; Poole, K. M.; Abboud, K. A.; Wernsdorfer, W.; O'Brien, T. A.; Christou, G. *Inorg. Chem.* **2008**, *47*, 5006–5021.
(12) Zaleski, C. M.; Weng, T.-C.; Dendrinou-Samara, C.; Alexiou, M.; Kanakaraki, P.; Hsieh, W.-Y.; Kampf, J.; Penner-Hahn, J. E.; Pecoraro, V. L.; Kessissoglou, D. P. *Inorg. Chem.* **2008**, *47*, 6127–6136.
(13) Bagai, R.; Abboud, K. A.; Christou, G. *Inorg. Chem.* **2008**, *47*, 621–631.
(14) Bhula, R.; Collier, S.; Robinson, W. T.; Weatherburn, D. C. *Inorg. Chem.* **1990**, *29*, 4027–4032.
(15) Bhula, R.; Gainsford, G. J.; Weatherburn, D. C. *J. Am. Chem. Soc.* **1988**, *110*, 7550–7552.
(16) Dimitrakopoulou, A.; Psycharis, V.; Raptopoulou, C. P.; Terzis, A.; Tangoulis, V.; Kessissoglou, D. P. *Inorg. Chem.* **2008**, *47*, 7608–7614.
(17) Lampropoulos, C.; Abboud, K. A.; Stamatatos, T. C.; Christou, G. *Inorg. Chem.* **2009**, *48*, 813–815.
(18) Maspoch, D.; Gómez-Segura, J.; Domingo, N.; Ruiz-Molina, D.; Wurst, K.; Rovira, C.; Tejada, J.; Veciana, J. *Inorg. Chem.* **2005**, *44*, 6936–6938.
(19) Sobota, P.; Utko, J.; Szafert, S.; Janas, Z.; Glowiak, T. *J. Chem. Soc., Dalton Trans.* **1996**, 3469–3473.
(20) Seela, J. L.; Knapp, M. J.; Kolack, K. S.; Chang, H.-R.; Huffman, J. C.; Hendrickson, D. N.; Christou, G. *Inorg. Chem.* **1998**, *37*, 516–525.
(21) Aromí, G.; Gamez, P.; Krzystek, J.; Kooijman, H.; Spek, A. L.; MacLean, E. J.; Teat, S. J.; Nowell, H. *Inorg. Chem.* **2007**, *46*, 2519–2529.

Published on Web 01/14/2010

being chemically equivalent. Asymmetric linear [Mn^{III}-$Mn^{III}Mn^{II}$] and [$Mn^{II}Mn^{II}Mn^{II}$] compounds have recently been reported, but are rare.[21,22] In the two referenced examples reported by Aromí et al., the manganese ions are bridged and oriented by long polydentate ligands.[21,22]

We report a novel complex of Mn(II) with bis(2-pyridylmethyl)-1,2-ethanediamine (bispicen).[26] Previously, the bispicen ligand has been used to prepare other polynuclear manganese cage complexes and three-dimensional structures.[27,28] The compound [Mn_3Cl_6(bispicen)$_2$] (**$Mn_3Cl_6L_2$**) serendipitously self-assembles from a 2:3 ratio of bispicen to $MnCl_2$ in acetonitrile. The compound is unusual in that it contains a highly asymmetric linear array of Mn(II) ions, with each metal ion in a different coordination environment. The reported synthesis demonstrates that specialized organic ligands are not strictly necessary for the stabilization and isolation of highly asymmetric manganese cage complexes.

Experimental Section

Materials. Ethylenediamine, 2-pyridinecarboxaldehyde, sodium borohydride ($NaBH_4$), methylene chloride (CH_2Cl_2), chloroform ($CHCl_3$), acetonitrile (MeCN), methanol (MeOH), sodium sulfate (Na_2SO_4), magnesium sulfate ($MgSO_4$), and manganese chloride ($MnCl_2$) were purchased from Sigma-Aldrich and used without further purification. Anhydrous diethyl ether (ether) was purchased from Fisher Scientific and stored over 4 Å molecular sieves. Ethanol (EtOH) was bought from Fluka and used as received. Tetrabutylammonium perchlorate (TBAP) was purchased from Sigma-Aldrich and stored in a glovebox free of moisture and oxygen. Chloroform-*d* and acetonitrile-d_3 were purchased from Cambridge Isotopes and used as received. The syntheses of *N,N*-bis(2-pyridylmethyl)-1,2-ethanediamine (bispicen)[26] and [Mn(bispicen)Cl_2][28,29] have been reported previously.

Synthesis. [Mn_3Cl_6(bispicen)$_2$] ($Mn_3Cl_6L_2$). An anaerobic solution of bispicen (0.3084 g, 1.273 mmol) in 20 mL of anhydrous MeCN was added to 0.2438 g of $MnCl_2$ (1.937 mmol). The resultant suspension was heated at 70 °C for 16 h. After cooling to 0 °C, 0.2950 g of the product was isolated as an off-white powder (53%). Crystals suitable for X-ray diffraction were grown through vapor diffusion of ether into a saturated solution of the powder in MeCN. Cyclic Voltammetry (MeCN): E_{pa} = +0.785 V versus SHE. Elemental Analysis: Calcd for $C_{28}Cl_6H_{36}Mn_3N_8 \cdot 2H_2O$: C, 37.44; H, 4.49; N, 12.48; Found: C, 37.24; H, 4.11; N, 12.34.

Instrumentation. All ^1H and ^{13}C nuclear magnetic resonance (NMR) spectra were recorded on a 400 MHz AV Bruker NMR spectrometer at 294 K and referenced to internal standards. A crystalline sample of **$Mn_3Cl_6L_2$** was dried and sent to Atlantic Microlabs (Norcross, GA) for the elemental analysis. Electron paramagnetic resonance (EPR) spectra were collected on a Bruker EMX-6/1 X-band EPR spectrometer in the perpendicular mode and analyzed with the program EasySpin.[30] Each sample was run as a frozen EtOH or MeCN solution in a quartz tube.

Table 1. Selected Crystallographic Data for **$Mn_3Cl_6L_2$**

parameter	
formula	$C_{28}H_{36}Cl_6Mn_3N_8$
MW	862.17
cryst syst	monoclinic
space group	$P2_1/n$ (No. 11)
a (Å)	20.560(2)
b (Å)	7.5778(9)
c (Å)	23.833(3)
α (deg)	90
β (deg)	101.031(2)
γ (deg)	90
V (Å^3)	3644.5(7)
Z	4
cryst color	colorless
T (K)	193
reflns collected	54847
unique reflns	15132
R1 (F, $I > 2\sigma(I)$)[a]	0.0394
wR2 (F^2, all data)[a]	0.0966

[a] $R1 = \sum||F_o| - |F_c||/\sum|F_o|$; $wR2 = [\sum w(F_o^2 - F_c^2)^2/\sum wF_o^4]^{1/2}$.

X-ray Crystallography. A crystal of **$Mn_3Cl_6L_2$** was mounted in paratone oil on a glass fiber and aligned on a Bruker SMART APEX CCD X-ray diffractometer. Graphite monochromated Mo Kα radiation (λ = 0.71073 Å) from a sealed tube and a monocapillary collimator were used for intensity measurements. SMART (v 5.624) was used to determine the preliminary cell constants and to control the data acquisition. The intensities of reflections of a sphere were collected by a combination of three sets of exposures (frames). Each set corresponded to a different ϕ angle for the crystal, and each exposure covered a range of 0.3° with respect to ω. A total of 1800 frames were collected with an exposure time of 40 s per frame. The data were corrected for Lorentz and polarization effects. The structure was solved using direct methods and expanded using Fourier techniques. All non-hydrogen atoms were refined anisotropically; whereas, each hydrogen atom was included at an idealized position 0.95 Å from its parent atom prior to the final refinement. Additional details regarding the data acquisition and analysis are included in Table 1 and in the files provided as Supporting Information.

Cyclic Voltammetry. Electrochemical measurements were recorded with a 300 mV/s scan rate under anaerobic conditions at 294 K. A Pine Instrument Co. AFCBP1 bipotentiostat, a platinum working electrode, a platinum wire auxiliary electrode, 0.10 M TBAP supporting electrolyte, and a silver wire reference electrode were used for cyclic voltammetry. All potentials were referenced to the ferrocenium/ferrocene couple (+0.590 V vs SHE in MeCN).[31] Each measurement was repeated at least three times, using freshly and independently prepared samples.

Magnetic Measurements. Magnetic susceptibility data were collected using a Quantum Design MPMS-XL SQUID magnetometer at temperatures ranging from 2 to 300 K under an applied field of 1000 G. Powdered samples were loaded into gelatin capsules and inserted into straws for analysis. Magnetization data were collected at temperatures ranging from 2 to 25 K under applied fields of 10, 20, 30, 40, and 50 kG. Samples for magnetization studies were encased in eicosane to prevent torquing of crystallites at high magnetic fields. Alternating current (AC) susceptibility data were collected at temperatures ranging from 2 to 5 K in a zero applied direct current (DC) field and a 1 G AC field oscillating at a frequency of 100 Hz. All data

(22) Aromí, G.; Berzal, P. C.; Gamez, P.; Roubeau, O.; Kooijman, H.; Spek, A. L.; Driessen, W. L.; Reedijk, J. *Angew. Chem., Int. Ed.* **2001**, *40*, 3444–3446.
(23) Li, X.; Kessissoglou, D. P.; Kirk, M. L.; Bender, C. J.; Pecoraro, V. L. *Inorg. Chem.* **1988**, *27*, 1–3.
(24) Tangoulis, V.; Malamatari, D. A.; Spyroulias, G. A.; Raptopoulou, C. P.; Terzis, A.; Kessissoglou, D. P. *Inorg. Chem.* **2000**, *39*, 2621–2630.
(25) Kessissoglou, D. P.; Kirk, M. L.; Lah, M. S.; Li, X.; Raptopoulou, C.; Hatfield, W. E.; Pecoraro, V. L. *Inorg. Chem.* **1992**, *31*, 5424–5432.
(26) Toftlund, H.; Pedersen, E.; Yde-Andersen, S. *Acta. Chem. Scand. A* **1984**, *38*, 693–697.
(27) Shaikh, N.; Panja, A.; Goswami, S.; Banerjee, P.; Vojtíšek, P.; Zhang, Y.-Z.; Su, G.; Gao, S. *Inorg. Chem.* **2004**, *43*, 849–851.
(28) Marvilliers, A.; Parsons, S.; Rivière, E.; Audière, J.-P.; Mallah, T. *Chem. Commun.* **1999**, 2217–2218.
(29) Chiswell, B. *Inorg. Chim. Acta* **1975**, *12*, 195–198.
(30) Stoll, S.; Schweiger, A. *J. Magn. Reson.* **2006**, *178*, 42–55.
(31) Zuman, P.; Meites, L. *Electrochemical Data*; John Wiley & Sons: New York, 1974.

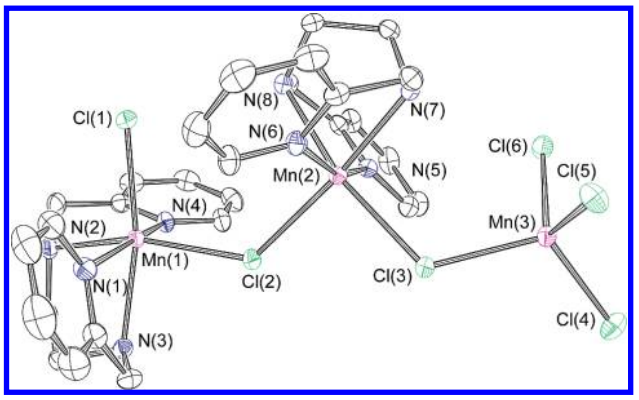

Figure 1. ORTEP representation of the crystal structure of $\mathbf{Mn_3Cl_6L_2}$. All thermal ellipsoids are drawn at 50% probability. Hydrogen atoms are omitted for clarity.

were corrected for diamagnetic corrections using Pascal's constants and by subtracting the diamagnetic susceptibility of an empty sample holder. Susceptibility data were fit to magnetic models with the programs julX and ANISOFIT.[32,33] Exchange coupling values are based on spin Hamiltonians with the general form $\hat{H} = -2J(\hat{S}_i \cdot \hat{S}_j)$.

Results

Synthesis. The formation of the trinuclear compound, $\mathbf{Mn_3Cl_6L_2}$, from $MnCl_2$ and bispicen requires prolonged heating at 70 °C. Over the course of the 16 h reaction, the product precipitates as a white powder. The trinuclear Mn(II) compound is less soluble in MeCN than both [Mn(bispicen)Cl_2], the probable initial complexation product of the reaction between the Mn(II) salt and ligand, and the starting material $MnCl_2$. The disappearance of the pinkish color associated with $MnCl_2$ provides a rough visual cue as to the progress of the reaction. After cooling the reaction mixture to 0 °C, $\mathbf{Mn_3Cl_6L_2}$ is obtained in modest yield (53%).

Crystal Structure. The trinuclear Mn(II) compound was crystallized via the slow diffusion of ether into a saturated MeCN solution. X-ray diffraction reveals three manganous ions, Mn(1−3), in a roughly linear array, with a Mn(1)−Mn(2)−Mn(3) angle of 146.53°. Two chloride anions connect the central Mn(2) to Mn(1) and Mn(3) (Table 1, Figure 1). The two Mn−Cl−Mn bridges are bent, with angles of 128.04(2)° and 116.688(18)° (Table 2). Direct intramolecular interaction between Mn(1) and Mn(3) is highly unlikely, for these metal ions are 8.357 Å apart. The chloride count requires a net +6 charge distributed among the three manganese ions to account for the molecule's neutrality. The Mn−N and Mn−Cl bonds surrounding Mn(1) and Mn(2) (Table 2) have lengths similar to those previously observed for hexacoordinate, high-spin Mn(II) centers.[34−39] The Mn−Cl bonds around Mn(3) have lengths typical for four-coordinate Mn(II) centers,[40−42] suggesting that this manganese ion is also divalent.

Table 2. Selected Bond Lengths and Angles for $\mathbf{Mn_3Cl_6L_2}$

bond	length (Å)	bond	length (Å)
Mn(1)−Cl(1)	2.4613(6)	Mn(2)−N(7)	2.2671(15)
Mn(1)−Cl(2)	2.5132(5)	Mn(2)−N(8)	2.3053(15)
Mn(1)−N(1)	2.2588(15)	Mn(3)−Cl(3)	2.4240(5)
Mn(1)−N(2)	2.2674(15)	Mn(3)−Cl(4)	2.3298(6)
Mn(1)−N(3)	2.2765(15)	Mn(3)−Cl(5)	2.3431(6)
Mn(1)−N(4)	2.2859(15)	Mn(3)−Cl(6)	2.3559(5)
Mn(2)−Cl(2)	2.4847(5)		
Mn(2)−Cl(3)	2.5485(5)	L−M−L	angle (deg)
Mn(2)−N(5)	2.2341(14)	Mn(1)−Cl(2)−Mn(2)	128.04(2)
Mn(2)−N(6)	2.2412(15)	Mn(2)−Cl(3)−Mn(3)	116.688(18)

Two equivalents of the tetradentate organic ligand *N*,*N*-bis(2-pyridylmethyl)-1,2-ethanediamine (bispicen) are present in the asymmetric unit with the three Mn(II) ions. Each bispicen binds to a single Mn(II) ion within the molecule in a *cis*-α conformation, with the pyridine rings *trans* to each other and the chloride anions *cis* to each other (Figure 1).[43−46] Unexpectedly, the bispicen ligands do not cap both termini of the cage, as is normally seen with 2:3 ligand/metal complexes with non-bridging polydentate ligands.[6,7] Instead, one bispicen coordinates to the central Mn(2) instead of Mn(3). This renders the molecule asymmetric, with each Mn(II) center in a unique coordination environment. Chloride anions complete an overall octahedral coordination for Mn(1) and Mn(2). Mn(3), conversely, is coordinated by a tetrahedral array of chloride ions.

In addition to the bridging chlorides Cl(2) and Cl(3), Mn(1) and Mn(3) are bound to one and three terminal chlorides, respectively. Considering each Mn(II) center separately, the bonds to the bridging chlorides are longer than those to the terminal chlorides (Table 2). Consistent with the change in coordination geometry, the Mn−Cl bonds around the tetracoordinate Mn(3) are much shorter than those around the octahedrally coordinated Mn(1) and Mn(2).[34]

Solution Characterization. Solutions of both powder and crystalline samples of the trinuclear species in MeCN display a single irreversible feature with an $E_{pa} = +785$ mV versus SHE (Figure 2). The cyclic voltammogram is distinct from both [Mn(bispicen)Cl_2] and $[MnCl_4]^{2-}$ (Supporting Information, Figure S1).[42] Frozen solutions

(32) Shores, M. P.; Sokol, J. J.; Long, J. R. *J. Am. Chem. Soc.* **2002**, *124*, 2279–2292.
(33) Bill, E., **2008**; http://ewww.mpi-muelheim.mpg.de/bac/logins/bill/julX_en.php.
(34) Shannon, R. D. *Acta Cryst.* **1976**, *A32*, 751–767.
(35) Triller, M. U.; Pursche, D.; Hsieh, W.-Y.; Pecoraro, V. L.; Rompel, A.; Krebs, B. *Inorg. Chem.* **2003**, *42*, 6274–6283.
(36) Coates, C. M.; Nelson, A.-G. D.; Goldsmith, C. R. *Inorg. Chim. Acta* **2009**, *362*, 4797–4803.
(37) Sjödin, M.; Gätjens, J.; Tabares, L. C.; Thuéry, P.; Pecoraro, V. L.; Un, S. *Inorg. Chem.* **2008**, *47*, 2897–2908.
(38) Wu, J.-Z.; Bouwman, E.; Mills, A. M.; Spek, A. L.; Reedijk, J. *Inorg. Chim. Acta* **2004**, *357*, 2694–2702.
(39) Romero, I.; Collomb, M.-N.; Deronzier, A.; Llobet, A.; Perret, E.; Pécaut, J.; Le Pape, L.; Latour, J.-M. *Eur. J. Inorg. Chem.* **2001**, *2001*, 69–72.
(40) Klein Gebbink, R. J. M.; Jonas, R. T.; Goldsmith, C. R.; Stack, T. D. P. *Inorg. Chem.* **2002**, *41*, 4633–4641.
(41) Zhang, H.; Chen, P.; Fang, L. *Acta Cryst., Sect. E* **2006**, *62*, m658–m660.
(42) Bhaduri, S.; Tasiopoulos, A. J.; Bolcar, M. A.; Abboud, K. A.; Streib, W. E.; Christou, G. *Inorg. Chem.* **2003**, *42*, 1483–1492.
(43) Arulsamy, N.; Goodson, P. A.; Hodgson, D. J.; Glerup, J.; Michelsen, K. *Inorg. Chim. Acta* **1994**, *216*, 21–29.
(44) Jo, D.-H.; Chiou, Y.-M.; Que, L., Jr. *Inorg. Chem.* **2001**, *40*, 3181–3190.
(45) Mialane, P.; Tchertanov, L.; Banse, F.; Sainton, J.; Girerd, J.-J. *Inorg. Chem.* **2000**, *39*, 2440–2444.
(46) White, M. C.; Doyle, A. G.; Jacobsen, E. N. *J. Am. Chem. Soc.* **2001**, *123*, 7194–7195.

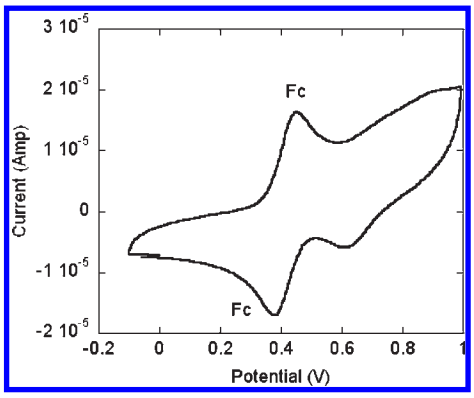

Figure 2. Cyclic voltammogram for $\mathbf{Mn_3Cl_6L_2}$ in a 0.10 M solution of tetrabutylammonium perchlorate in acetonitrile. Ferrocene (Fc) is added as an internal standard. The cyclic voltammogram of [Mn(bispicen)Cl_2] in MeCN is provided in the Supporting Information for comparative purposes.

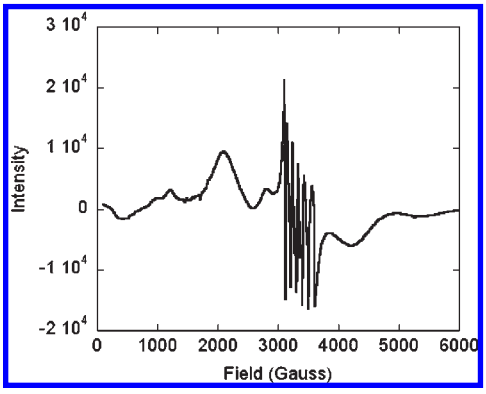

Figure 3. X-band EPR spectrum of a 5 mM sample $\mathbf{Mn_3Cl_6L_2}$ in EtOH at 77 K.

of $\mathbf{Mn_3Cl_6L_2}$ in MeCN and EtOH were studied by EPR at 77 K. The EPR spectrum in MeCN (Supporting Information, Figure S3) displays a broad signal because of the poor solubility of $\mathbf{Mn_3Cl_6L_2}$ in MeCN and the solvent's limited capacity to glass. The EPR data for the trinuclear species in EtOH (Figure 3) are consistent with the presence of at least two manganese species, indicating that $\mathbf{Mn_3Cl_6L_2}$ does not retain its solid-state structure in this solvent.

Magnetic Properties. A plot of $1/\chi$ versus T shows a linear relationship as predicted by the Curie−Weiss law with a negative Weiss constant, which is consistent with net antiferromagnetic coupling in the compound (see Supporting Information for details).

A plot of $\chi_M T$ versus T is shown in Figure 4. The $\chi_M T$ value at 300 K (13.03 emu·K·mol^{-1}) is very close to, but slightly smaller than, that predicted for three non-interacting high-spin Mn(II) ions (13.125 emu·K·mol^{-1}). As the temperature cools to 50 K, the value of $\chi_M T$ decreases gradually; further cooling causes $\chi_M T$ to decrease more rapidly to a minimum of 3.52 emu·K·mol^{-1}at 2 K. This value is smaller than that predicted for the $S = {}^5/_2$ ground state anticipated for three antiferromagnetically coupled Mn(II) ions (4.375 emu·K·mol^{-1}), which may indicate either intermolecular interactions or perhaps the population of low-lying excited spin states.

Initial fits to the susceptibility data were attempted using julX and the Hamiltonian for a non-symmetrical

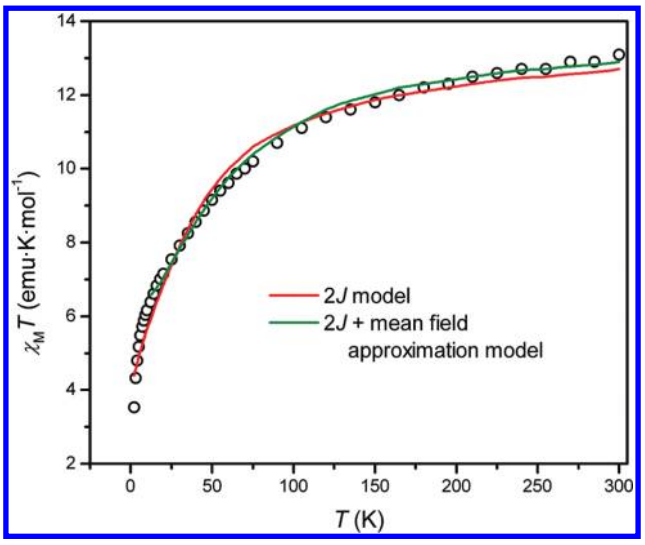

Figure 4. Magnetic behavior of $\mathbf{Mn_3Cl_6L_2}$ as measured at 1000 G. The solid lines represent calculated fits to the data; see text for details.

trinuclear complex: $\hat{H} = -2J_{12}(\hat{S}_1 \cdot \hat{S}_2) - 2J_{23}(\hat{S}_2 \cdot \hat{S}_3) - 2J_{13}(\hat{S}_1 \cdot \hat{S}_3)$.[47] The most conservative fit (red trace, Figure 4) assumes that only coupling between adjacent spin centers is operative, with $J_{13} = 0$. Here, the best fit gives $J_{12} = -3.23$ cm^{-1} and $J_{23} = 0.63$ cm^{-1}, with all g values fixed at 2.00, and a fixed temperature-independent paramagnetism (TIP) value standard for three first-row transition metal ions (600×10^{-6} emu·mol^{-1}). The associated f value (sum of the squared deviations) equals 0.3401. The Supporting Information provides a more detailed explanation of the fitting procedure. On the basis of the J_{12} value, the interaction between Mn(1) and Mn(2) is predominantly antiferromagnetic; conversely, that between Mn(2) and Mn(3) is weakly ferromagnetic.

The simple fit follows the gross features of the susceptibility data; however, visual inspection makes obvious the need for additional fitting parameters. We first consider *inter*molecular magnetic interactions. The trinuclear species has hydrogen bonding pathways in two directions (Figure 5): an NH moiety on Mn(1) can interact with the Cl^- on a neighboring Mn(3) to give chains of clusters and a potential intermolecular $J_{13'}$ coupling constant, while the Cl^- on Mn(1) can interact with an NH moiety on a neighboring Mn(1) to give a 2D net of clusters and a potential intermolecular $J_{11'}$ coupling constant. There is ample literature precedence for invoking magnetic exchange via H-bonding interactions.[28,38,48]

The molecular field approximation was utilized to model intercluster interactions.[49] The susceptibility for the trinuclear complex is corrected using the formula:

$$\chi_{\text{corr.}} = \frac{\chi_{\text{tri}}}{1 - \chi_{\text{tri}} \dfrac{2zJ'}{Ng^2\beta^2}}$$

where z is the number of interacting nearest neighbors and J' is the intermolecular coupling constant. With this correction, an improved fit ($f = 0.1277$, green trace in

(47) Kahn, O. *Molecular Magnetism*; VCH: New York, NY, 1993.
(48) Yan, B.; Wang, S.; Chen, Z. *Monatsh. Chem.* **2001**, *132*, 305–314.
(49) O'Connor, C. J. *Prog. Inorg. Chem.* **1982**, *29*, 203–283.

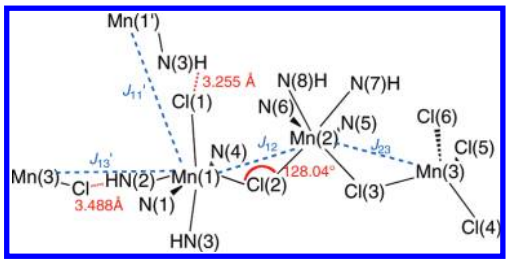

Figure 5. Schematic of potential coupling pathways shown as blue dashed lines. Hydrogen bonds between the cluster and neighboring complexes are shown as red dashed lines.

Figure 4) is obtained, which yields $J_{12} = -6.0\ cm^{-1}$, $J_{23} = 3.5\ cm^{-1}$, and $zJ' = 0.42\ cm^{-1}$, with all g values fixed at 2.00 and TIP set at 600×10^{-6} emu·mol^{-1}. The positive value of zJ' suggests an overall ferromagnetic interaction through the hydrogen bonds. The small magnitude of zJ' indicates that either the intermolecular interactions are extremely weak or the ferro- and antiferromagnetic intercluster exchanges largely cancel each other. The fit is satisfactory down to 10 K. Below this temperature, the small J values likely lead to a poorly isolated ground state and a potential for magnetic anisotropy (D) that may be responsible for the more rapid downturn in $\chi_M T$.[50]

Magnetization data (Supporting Information, Figure S5 inset) suggest the presence of magnetic anisotropy (D), as the magnetization values of isofield data are not superimposable and do not fit the expected Brillouin function for either of the possible ground states of $S = {}^5/_2$ or $S = {}^{15}/_2$. Although not saturated even at 50 kG, the magnetization achieves a value of 7.94 μ_B at 2 K and 50 kG. This indicates that even at high field and low temperature, the ground state is not well-isolated and low-lying excited states of differing spin are present. Not surprisingly, attempts to fit the data using ANISOFIT provide extremely poor fits. Attempts to fit the susceptibility with a "2J plus anisotropy model" using julX provide comparable fits to the model described above (see Supporting Information for details), but yield D values that are unreasonably large for normally isotropic high-spin d^5 ions, even for a complex with such anisotropic geometry as encountered in **$Mn_3Cl_6L_2$**.

We note that neither in-phase nor out-of-phase peaks are observed in an initial study of the variable temperature AC susceptibility, indicating that this complex does not exhibit slow relaxation of the magnetization, and therefore cannot be classified as a SMM.

Discussion

The trinuclear manganous compound $[Mn_3Cl_6(bispicen)_2]$ (**$Mn_3Cl_6L_2$**) is produced at moderate (53%) yield during the prolonged heating of a 2:3 mixture of bispicen and $MnCl_2$ in acetonitrile. The reaction appears to be kinetically driven by the reduced solubility of **$Mn_3Cl_6L_2$** relative to the starting materials and lower nuclearity intermediates. The mononuclear $[Mn(bispicen)Cl_2]$ has been previously reported and is likely the initial product from the reaction between the organic ligand and $MnCl_2$.[28,29] We speculate that two of these mononuclear species combine to form a second intermediate, $[Mn_2Cl_4L_2]$, perhaps with a chemically precedented Mn(II)$_2$Cl$_2$ diamond core.[27] The asymmetric addition of $MnCl_2$ to the binuclear intermediate would yield **$Mn_3Cl_6L_2$**.

The trinuclear product has an unusual asymmetric structure with scant chemical precedence.[21,22] The metal−ligand bond distances (Table 2) and the anion count are consistent with three Mn(II) ions in the structure.[34] The Mn(II) ions are arrayed linearly with a single chloride anion linking each pair of adjacent metal ions. The asymmetry results from the different coordination spheres around the terminal Mn(II) ions (Figure 1). One is hexacoordinate, being bound to one tetradentate bispicen ligand, a terminal chloride, and a bridging chloride. The other terminal Mn(II) is tetracoordinate, with bonds to three terminal chlorides and a bridging chloride. The bond lengths between the Mn(II) ions and the bridging chlorides (Table 2) are shorter than those previously reported.[27,39] In these prior examples, the pairs of manganous ions are connected via two chloride anions, not one, providing a rationale for the shorter Mn−Cl bonds observed for **$Mn_3Cl_6L_2$**.

The success of the synthesis, while serendipitous, demonstrates that asymmetric polynuclear metal compounds do not require ligands capable of spanning and orienting multiple metal ions. Each of the two bispicen ligands in **$Mn_3Cl_6L_2$** binds to only one manganous ion.

The chemical and physical properties of **$Mn_3Cl_6L_2$** have been investigated through cyclic voltammetry, EPR, and variable temperature magnetic susceptibility. The electrochemistry in MeCN displays a single irreversible feature (Figure 2), which may correspond to the oxidation of the $[Mn(II)_3]$ complex to a $[Mn(II)_2Mn(III)]$ species. This feature is distinct from those observed for $[Mn(bispicen)Cl_2]$ and $[MnCl_4]^{2-}$.[42] The EPR spectrum of the compound in MeCN (Supporting Information, Figure S3) displays an extremely broadened signal that could correspond to either a single or multiple manganese species. The EPR data for the trinuclear manganese compound in EtOH (Figure 3) are consistent with multiple species, one of which appears to be mononuclear. The compound loses its structural integrity upon solvation in EtOH; whether it does so in MeCN remains unresolved.

Antiferromagnetism would be anticipated given the geometry and the chemical makeup of the bridges between the Mn(II) ions.[51−54] Net antiferromagnetic coupling is confirmed by variable temperature magnetic susceptibility studies. The $\chi_M T$ value at 300 K is consistent with three noninteracting Mn(II) ions. Conversely, the measured $\chi_M T$ at 2 K is slightly lower than that predicted for three antiferromagnetically coupled manganous ions.

Preliminary analysis of the data with the julX program suggests that Mn(1) and Mn(2) interact antiferromagnetically. In contrast, a weak ferromagnetic interaction exists between Mn(2) and the tetrahedrally coordinated Mn(3). Antiferromagnetic coupling between the octahedral Mn(II) ions (J_{12}, Figure 5) is expected based on the obtuse Mn−Cl−Mn bond angle of 128.04(2)°. This geometry allows

(50) Xu, J.-X.; Ma, Y.; Liao, D.-z.; Xu, G.-F.; Tang, J.; Wang, C.; Zhou, N.; Yan, S.-P.; Cheng, P.; Li, L.-C. *Inorg. Chem.* **2009**, *48*, 8890–8896.

(51) Boersma, F.; Tinus, A. M. C.; Kopinga, K.; Paduan-Filho, A.; Carlin, R. L. *Physica B+C* **1982**, *114*, 231–237.

(52) Kobayashi, H.; Tsujikawa, I.; Friedberg, S. A. *J. Low Temp. Phys.* **1973**, *10*, 621–633.

(53) Martin, J. D.; Hess, R. F.; Boyle, P. D. *Inorg. Chem.* **2004**, *43*, 3242–3247.

(54) Simizu, S.; Chen, J.-Y.; Friedberg, S. A. *J. Appl. Phys.* **1984**, *55*, 2398–2400.

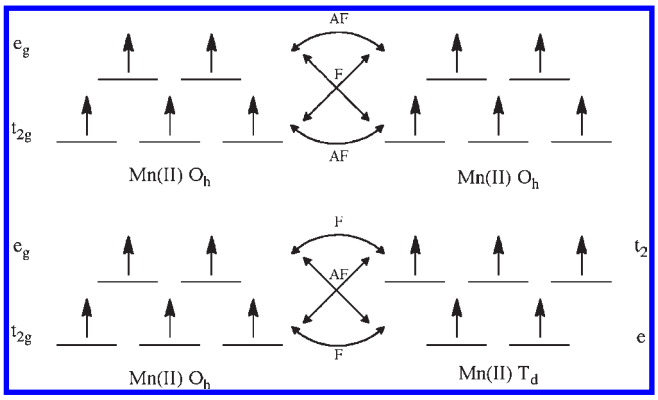

Figure 6. Ferromagnetic and antiferromagnetic coupling for Mn(II) ions based on orbital overlap between octahedral-octahedral (top) and octahedral-tetrahedral (bottom) energy levels.

significant orbital overlap between the Mn 3d orbitals and the Cl 3p orbitals, enabling an antiferromagnetic superexchange pathway.[53] The strength of the coupling is comparable to that observed in similar chloride-bridged Mn(II) complexes.[51,52,54] Conversely, the weaker ferromagnetic coupling between octahedral and tetrahedral Mn(II) ions (J_{23}) is consistent with orbital orthogonality arising from the different geometries of Mn(2) and Mn(3). The overlap between the tetrahedral Mn d orbitals and the Cl p orbitals is much weaker than for the octahedral Mn ion, therefore minimizing antiferromagnetic interactions. Meanwhile, the inverted orbital arrangement (see Figure 6) leads to a better energy match between the e- and t_2-type orbitals, which enables a degree of ferromagnetic coupling.

Attempts to improve the fit are complicated by the presence of low-energy excited states and/or intermolecular interactions. Although a good fit to the susceptibility data can be obtained by considering intramolecular coupling between neighboring manganese atoms combined with single-ion anisotropy (D), the calculated anisotropy values are unreasonable and overparameterization is likely. A modeling approach that disregards anisotropy but instead considers intermolecular interactions satisfactorily fits the data but fails to provide a comprehensive model that fully accounts for the low-temperature magnetization behavior. The weak nearest neighbor coupling proposed for $\mathbf{Mn_3Cl_6L_2}$ is common for Mn(II)-containing species and should facilitate the population of magnetic excited states.[10,24,25] The current model confirms the anticipated superexchange pathways, which endow $\mathbf{Mn_3Cl_6L_2}$ with an $S = {}^5/_2$ ground state.

Conclusion

The reported synthesis of $\mathbf{Mn_3Cl_6L_2}$, while serendipitous, demonstrates that asymmetric trinuclear manganese complexes can assemble without the benefit of a complex ligand capable of bridging all three metal ions. The magnetic properties of $\mathbf{Mn_3Cl_6L_2}$ are consistent with an $S = 5/2$ system, indicating that the interactions between the three Mn(II) ions are largely antiferromagnetic. A more detailed analysis of the magnetic susceptibility data suggest that the interaction between the two octahedrally coordinated Mn(II) ions is antiferromagnetic; whereas, that between Mn(2) and the tetrahedrally coordinated Mn(3) is weakly ferromagnetic.

Acknowledgment. This research was funded by Auburn University and Colorado State University. The authors are grateful to Dr. Evert Duin (Auburn University) for his assistance with the acquisition of the EPR data and thank Mr. J. Allison and Prof. A. K. Rappé (CSU) for helpful discussions relating to magnetic property modeling. The authors also thank the reviewers for their insightful suggestions.

Supporting Information Available: Additional information as noted in the text. This material is available free of charge via the Internet at http://pubs.acs.org.